Peptides 33 (2012) 9–17

Contents lists available at SciVerse ScienceDirect

Peptides

journal homepage: www.elsevier.com/locate/peptides

Peptidotriazoles with antimicrobial activity against bacterial and fungal plant pathogens

Imma Güell[a], Lluís Micaló[a], Laura Cano[a], Esther Badosa[b], Rafael Ferre[a], Emilio Montesinos[b], Eduard Bardají[a], Lidia Feliu[a,*], Marta Planas[a,*]

[a] LIPPSO, Department of Chemistry, University of Girona, Campus Montilivi, E-17071 Girona, Spain
[b] Laboratory of Plant Pathology, Institute of Food and Agricultural Technology-CIDSAV-XaRTA, University of Girona, Campus Montilivi, 17071 Girona, Spain

ARTICLE INFO

Article history:
Received 8 November 2011
Received in revised form 7 December 2011
Accepted 7 December 2011
Available online 16 December 2011

Keywords:
Antimicrobial peptides
Click reaction
Peptidomimetics
Heterocyclic peptides

ABSTRACT

We designed and prepared peptidotriazoles based on the antimicrobial peptide BP100 (LysLysLeuPheLysLysIleLeuLysTyrLeu-NH_2) by introducing a triazole ring in the peptide backbone or onto the side chain of a selected residue. These compounds were screened for their in vitro growth inhibition of bacterial and fungal phytopathogens, and for their cytotoxic effects on eukaryotic cells and tobacco leaves. Their proteolytic susceptibility was also analyzed. The antibacterial activity and the hemolysis were influenced by the amino acid that was modified with the triazole as well as by the absence of presence of a substituent in this heterocyclic ring. We identified sequences active against the bacteria *Xanthomonas axonopodis* pv. *vesicatoria*, *Erwinia amylovora*, *Pseudomonas syringae* pv. *syringae* (MIC of 1.6–12.5 μM), and against the fungi *Fusarium oxysporum* (MIC < 6.2–12.5 μM) with low hemolytic activity (0–23% at 50 μM), high stability to protease digestion and no phytotoxicity. These peptidotriazoles constitute good candidates to design new antimicrobial agents.

1. Introduction

Bacterial plant diseases play a significant role in crop losses in agriculture and their control is mainly achieved by treatments with copper compounds and antibiotics [1]. Although antibiotics are highly efficient in plant disease control, it has been reported the emergence of antibiotic-resistant strains and their use is hampered by environmental concerns. Therefore, the search for novel antimicrobial agents has been undertaken [26,30,41,46]. Antimicrobial peptides have emerged as promising agents to fight bacterial and fungal plant diseases of economic importance [28,33].

Antimicrobial peptides are components of the innate immune system found in a wide range of organisms, including microorganisms, plants, insects, amphibians and humans. Their mechanism of action has not been completely elucidated, however it has been postulated that they work primarily by compromising the membrane of the target organism [6,17,21,28]. This mechanism does not involve specific organization of their sequence or structure and, therefore, several diverse architectures have evolved. Despite this diversity, these sequences meet two common and functionally important requirements: most of them are cationic and are able to assume an amphipathic structure. It is generally accepted that the positive charge allows the electrostatic attraction of antimicrobial peptides with phospholipid membranes. Peptides are then prompted to adopt an amphipathic conformation that favors the insertion of their hydrophobic face into the membrane bilayer.

Despite the existence of natural potent antimicrobial peptides, they usually have long amino acid sequences, display poor bioavailability, are prone to protease degradation and might be toxic to animals and plants. To overcome these limitations, the development of de novo designed peptides has been carried out in order to identify compounds with remarkable biological activity [24,29,33,34]. One strategy that can be used to improve the biological profile of antimicrobial peptides is the introduction in their sequence of nitrogen heterocycles which play an important role in biological systems. Among them, 1,2,3-triazoles have been shown to possess a number of desirable features in drug discovery. This ring is chemically stable to acidic and basic hydrolysis as well as to reductive and oxidative conditions, and it is relatively resistant to metabolic degradation [39,44,45]. Moreover, 1,2,3-triazoles have a high dipole moment (about 5 D), being able to participate in hydrogen bonding and in dipole–dipole and π-stacking interactions. Consequently, this ring can interact with biological molecules and has been described as a powerful pharmacophore [3,13,25,27,37,44,45,47,48], and employed as bioisoster of potentially labile functional groups (e.g., esters, amides) [12,19,35].

The synthesis of 1,2,3-triazoles can be conveniently achieved by a copper(I)-catalyzed Huisgen 1,3-dipolar azide–alkyne cycloaddition [31]. This reaction is highly chemoselective, tolerates a variety

* Corresponding authors. Tel.: +34 972 418274; fax: +34 972 418150.
E-mail addresses: lidia.feliu@udg.edu (L. Feliu), marta.planas@udg.edu (M. Planas).

0196-9781/$ – see front matter © 2011 Elsevier Inc. All rights reserved.
doi:10.1016/j.peptides.2011.12.003

of functionalities and is carried out under mild conditions with quantitative conversions. Moreover, it has been established that it exclusively affords 1,4-disubstituted 1,2,3-triazoles in very good yields irrespective of the substituent on the alkyne [11,18,39]. It is therefore not surprising that it has been adapted to solid support, especially to obtain peptide derivatives [25,42]. In particular, it has been described its application to the solid-phase synthesis of β-turn mimics, protease inhibitors [43,44], cyclopeptide analogs [8,22,25,39,40], assembled and scaffolded peptides [15] or PEGylated lipopeptides [23]. In these reports, the azide–alkyne cycloaddition is employed to introduce the 1,2,3-triazole unit in the peptide backbone or at the side-chain of an amino acid as a ligation technique for linking peptide fragments for macrocyclization and polymerization, or to obtain biologically active peptidotriazoles [10,47].

Previously we have developed linear undecapeptides which inhibited the plant pathogenic bacteria *Erwinia amylovora*, *Xanthomonas axonopodis* pv. *vesicatoria*, and *Pseudomonas syringae* pv. *syringae*, and the plant pathogenic fungi *Penicillium expansum* and *Fusarium oxysporum* [4,5,14]. One of the best peptides, LysLysLeuPheLysLysIleLeuLysTyrLeu-NH_2 (**BP100**), also showed minimized cytotoxicity and low susceptibility to protease degradation. In our efforts to further improve the biological profile of **BP100**, we decided to study the effect of incorporating a 1,2,3-triazole ring in its structure.

Herein, we describe the design of analogs bearing a triazole in the peptide backbone or onto the side chain of a selected residue of **BP100**. For the latter, we studied the influence of modifying the side chain functionality of each polar residue (Lys) and of the hydrophobic aromatic amino acid (Phe) with a triazole moiety. We report the solid-phase synthesis of the peptidotriazoles, their screening for in vitro growth inhibition of bacterial and fungal phytopathogens, and for their cytotoxic effects on eukaryotic cells and tobacco leaves, as well as the analysis of their proteolytic susceptibility.

2. Material and methods

2.1. Materials

The 9-fluorenylmethoxycarbonyl (Fmoc) derivatives and Fmoc-Rink-4-methylbenzhydrylamine (MBHA) resin (0.56 mmol/g) were obtained from Senn Chemicals International (Gentilly, France) or from IRIS Biotech GmbH (Marktredwitz, Germany). Oxyma pure was purchased from Novabiochem (Nottingham, UK). Dicyclohexylammonium *N*-*tert*-butyloxycarbonyl-2-amino-6-azidohexanoate (Boc-Ahx(N_3)–OH), propiolic acid, trifluoroacetic acid (TFA), triisopropylsilane (TIS), benzyl azide (BnN_3), PPh_3, iodine, imidazole, ascorbic acid, CuI, and *N*,*N*′-diisopropylcarbodiimide (DIPCDI) were from Sigma–Aldrich Corporation (Madrid, Spain). Piperidine, sodium *N*,*N*-diethyldithiocarbamate and NaN_3 were purchased from Fluka (Buchs, Switzerland). Silica gel was from Merck (Nottingham, UK). *N*-Methyl-2-pyrrolidinone (NMP), *N*,*N*-dimethylformamide (DMF), CH_3OH, CH_2Cl_2, diethyl ether, ethyl acetate, hexane and solvents for reverse-phase high performance liquid chromatography (RP-HPLC) were obtained from Scharlau (Sentmenat, Spain).

2.2. General method for solid-phase peptide synthesis

All peptides were synthesized manually by the solid-phase method using Fmoc-type chemistry, and Boc or 4-methyltrityl (Mtt) side-chain protection for Lys and *tert*-butyl (*t*Bu) for Tyr. Fmoc-Rink-MBHA resin (0.56 mmol/g) was used as solid support to obtain C-terminal peptide amides. Couplings of the Fmoc-amino acids (4 equiv.) were mediated by Oxyma pure (4 equiv.) and DIPCDI (4 equiv.) in DMF for 1 h, and monitored by ninhydrin test. Fmoc group was removed by treating the resin with a mixture of piperidine – DMF (3:7; 2 + 10 min). Washings were performed with DMF (6×1 min) and CH_2Cl_2 (6×1 min). Peptide elongation was performed by repeated cycles of Fmoc group removal, coupling and washings.

Once the synthesis was completed, the peptidotriazoles were individually cleaved from the resin with TFA–H_2O–TIS (95:2.5:2.5). Following TFA evaporation and diethyl ether extraction, the crude peptidotriazoles were dissolved in H_2O, lyophilized and tested for purity on RP-HPLC performed at 1.0 mL/min. Linear gradients of 0.1% aqueous TFA and 0.1% TFA in CH_3CN were run from 0.98:0.02 to 0:1 over 7 min using a Kromasil (4.6 mm × 40 mm; 3.5 μM particle size) C_{18} reverse-phase column (method A) and over 28 min using a Ultrabase column (4.6 mm × 250 mm; 5 μM particle size) (method B) with UV detection at 220 nm. Electrospray ionization mass spectrometry (ESI-MS), high resolution mass spectrometry (HRMS (ESI)) and nuclear magnetic resonance (NMR) were used to confirm peptidotriazole identity.

2.3. Synthesis of peptidotriazoles ***BP135*** and ***BP136*** incorporating a triazole in the peptide backbone

2.3.1. Synthesis of Fmoc-Ile-Ψ[CH_2N_3]

Fmoc-Ile-Ψ[CH_2N_3] was synthesized starting from Fmoc-isoleucinol [38] as described by Mondal and Fan [32]. Briefly, Fmoc-isoleucinol (1.0 g, 2.95 mmol) in dry CH_2Cl_2 (12 ml) was added to a solution of PPh_3 (2.34 g, 8.93 mmol), iodine (2.26 g, 8.93 mmol) and imidazole (1.0 g, 14.88 mmol) in dry CH_2Cl_2 (30 ml) under nitrogen. The resulting mixture was stirred at room temperature for 2 h. After this time, the solvent was evaporated at reduced pressure and the residue was purified by silica gel column chromatography. Elution with ethyl acetate/hexane (1:4) afforded Fmoc-Ile-Ψ[CH_2I] (1.23 g, 93% yield) as a white solid. This iodide (800 mg, 1.78 mmol) and NaN_3 (579 mg, 8.90 mmol) were dissolved in DMF (8 ml) and stirred under nitrogen at room temperature for 5 h. After reaction completion, cold water was added and a precipitate was formed which was filtered, dried, and purified by silica gel column chromatography. Elution with ethyl acetate/hexane (1:4) afforded Fmoc-Ile-Ψ[CH_2N_3] (614 mg, 94% yield) as a white solid.

2.3.2. Solid-phase synthesis of ***BP135*** and ***BP136***

Peptidyl resins Fmoc-Tyr(*t*Bu)-Leu-Rink-MBHA (20 mg) and Fmoc-Lys(Boc)-Tyr(*t*Bu)-Leu-Rink-MBHA (20 mg) were prepared following the general procedure described above. After Fmoc removal, the N-terminal group was acylated with propiolic acid. Formation of the triazole ring was accomplished by treating the resulting peptidyl resins with Fmoc-Ile-Ψ[CH_2N_3] (25 mg, 5 equiv.), ascorbic acid (12.09 mg, 5 equiv.), and CuI (13.07 mg, 5 equiv.) in piperidine/DMF (2:8) for 5 h at room temperature. The peptide chain was then elongated with the corresponding amino acids. Acidolytic cleavage of the resins afforded the peptidotriazoles **BP135** and **BP136** in 98 and 85% purity, respectively.

2.4. Synthesis of peptidotriazoles ***BP238***–***BP250*** incorporating a triazole onto an amino acid side chain

Peptidyl resins containing an N^{ε}-Mtt-protected Lys or a propargylglycine were prepared following the general procedure described above. Once chain assembly was completed, peptidyl resins containing an N^{ε}-Mtt-protected Lys were treated with 1% TFA in CH_2Cl_2 upon which the solution became yellow. Each mixture was stirred for 5 min and the resins were then washed with CH_2Cl_2 (2×1 min), MeOH (2×1 min) and CH_2Cl_2 (2×1 min). TFA treatment and washes were repeated until the solution remained

colorless. Then, the N^{ε}-amino group was acylated with propiolic acid under the standard coupling conditions.

Each of the alkynyl resins were treated with the corresponding azide (NaN_3, Boc-Ahx(N_3)–OH or BnN_3) in the presence of ascorbic acid and CuI in piperidine/DMF (2:8), as described above. The reaction mixture was stirred overnight at room temperature. The resin was subsequently washed with sodium *N*,*N*-diethyldithiocarbamate (0.03 M in NMP, 3 × 15 min), DMF (6 × 1 min) and CH_2Cl_2 (1 × 20 min). Peptidotriazoles were individually cleaved from the resin with TFA–H_2O–TIS (95:2.5:2.5) and analyzed by RP-HPLC, mass spectrometry and NMR. Peptidotriazoles were obtained in purities ranging from 65 to 92%.

2.5. Bacterial strains and growth conditions

The following plant pathogenic bacterial strains were used: *E. amylovora* PMV6076 (Institut National de la Recherche Agronomique, Angers, France), *P. syringae* pv. *syringae* EPS94 (Institut de Tecnologia Agroalimentària, Universitat de Girona, Spain) and *X. axonopodis* pv. *vesicatoria* 2133-2 (Instituto Valenciano de Investigaciones Agrarias, Valencia, Spain). All bacteria were stored in Luria Bertani (LB) broth supplemented with glycerol (20%) and maintained at −80 °C. *E. amylovora* and *P. syringae* pv. *syringae* were scrapped from LB agar after growing for 24 h and *X. axonopodis* pv. *vesicatoria* after growing for 48 h at 25 °C. The cell material was suspended in sterile water to obtain a suspension of 10^8 CFU ml^{-1}.

2.6. Fungal strains and growth conditions

The plant pathogenic fungal strains *P. expansum* EPS 26 (INTEA, University of Girona) and *F. oxysporum* f. sp. *lycopersici* FOL 3 race 2 (ATCC 201829, American Type Culture Collection) were used. Strains were cultured on potato dextrose agar (PDA) plates (Difco) using aseptic procedures to avoid contamination. Conidia from *P. expansum* mycelium were obtained from 5-day-old PDA cultures of the fungus incubated at 25 °C. Inoculum was prepared by scraping spore material from the culture surfaces with a wet cotton swab and resuspending it in distilled water containing 0.5‰ of Tween 80. Microconidia of *F. oxysporum* were obtained from 1-week-old potato dextrose broth (PDB) cultures (Oxoid) of the fungus incubated at 25 °C in the dark in a rotary shaker at 125 rpm. After incubation, the culture was filtered through several layers of sterile cheesecloth to eliminate macroconidia and mycelial growth of the fungus. Then, the effluent was centrifuged at 8000 × *g* for 20 min at 4 °C, and the pellet was resuspended in sterile water. The concentration of conidia was determined using a hemacytometer and adjusted to 10^4 conidia ml^{-1} for *F. oxysporum* and 10^3 conidia ml^{-1} for *P. expansum*.

2.7. Antibacterial activity assays

Lyophilized peptidotriazoles were solubilized in sterile Milli-Q water to a final concentration of 1 mM and filter sterilized through a 0.22-μm pore filter. For MIC assessment, dilutions of the peptidotriazoles were made to obtain final concentrations of 500, 250, 125, 62.5, 31.2, 15.6 μM. Bacterial growth was automatically determined by optical density measurement at 600 nm as previously described [5,14]. The experiment was repeated twice. The MIC was taken as the lowest peptide concentration with no growth at the end of the experiment.

2.8. Antifungal activity assays

Lyophilized peptidotriazoles were solubilized in sterile Milli-Q water to a final concentration of 1 mM and filter sterilized through a 0.22-μm pore filter. For MIC assessment, stock solutions of peptidotriazoles were made to obtain final concentrations of 500, 250, 125, and 62.5 μM. Microbial growth was automatically determined by optical density measurement at 600 nm as previously described [4]. The MIC was taken as the lowest peptide concentration without growth at the end of the experiment.

2.9. Hemolytic activity

The hemolytic activity of peptides was evaluated at 50 and 150 μM. Hemoglobin release from erythrocyte suspensions of fresh human blood (5%, vol/vol) was determined using absorbance at 540 nm as previously described [5,14].

2.10. Cytotoxicity by a peptidotriazole infiltration assay

Peptidotriazole solutions of 25 and 50 μM concentration in H_2O were prepared and infiltrated (100 μL) into the mesophylls of fully expanded tobacco leaves using a syringe without a needle. Three infiltrations were done for each peptide at each concentration. Control infiltrations with water (negative control) or mellitin (positive control) at the same molar concentration were performed. The appearance of symptoms on the leaves was followed for 48 h after infiltration.

2.11. Susceptibility to protease degradation

Digestion of the peptides were carried out by treating 100 μg/ml peptide with 2 μg/ml proteinase K (Sigma–Aldrich Corporation, Madrid, Spain) in 100 mM TRIS buffer, pH 7.6, at room temperature. The peptide cleavage after 5, 10, 15, 30, 45 and 60 min was monitored by RP-HPLC as previously described [16]. The digestion was estimated as the percentage of degraded peptide calculated from the decrease of the RP-HPLC peak area of the native peptide.

3. Results

3.1. Design and synthesis of the peptidotriazoles

Peptides bearing a triazole at the backbone or at the side chain of a selected residue were designed based on the structure of **BP100** (LysLysLeuPheLysLysIleLeuLysTyrLeu-NH_2) (Fig. 1, Table 1). Peptidotriazoles were synthesized on solid phase following a standard Fmoc/*t*Bu strategy using Oxyma and DIPCDI for the coupling of the Fmoc-amino acids and a mixture of piperidine-DMF for the Fmoc removal. After the synthesis, the cleavage of the peptidotriazoles was performed with TFA–H_2O–TIS.

The **BP100** analogs bearing a triazole moiety in the peptide backbone were designed by replacing Ile^7-Leu^8 (**BP135**) and Leu^8-Lys^9 (**BP136**) with Ile-Ψ[CH_2triazoleCO]. The key step of the synthesis was the cycloaddition reaction between the corresponding alkynyl resin and Fmoc-Ile-Ψ[CH_2N_3] (Scheme 1). **BP135** and **BP136** are denoted as Ile^7-Tr and Ile^8-Tr, respectively, that stand for Ile-Ψ[CH_2triazoleCO].

Peptidotriazoles **BP238**–**BP247** were obtained by modifying each Lys residue of **BP100** with an unsubstitued triazole or with a triazole bearing a 2-aminohexanoic acid (Ahx). The synthesis was achieved by acylating the N^{ε}-amino group of a Lys residue with propiolic acid followed by cycloaddition with NaN_3 or Boc-Ahx(N_3)–OH (Scheme 2).

Substitution of the benzene ring of the Phe residue in **BP100** by an unsubstituted triazole or by a triazole substituted with a 2-aminohexanoic acid or with a benzyl group afforded peptidotriazoles **BP248**, **BP249**, and **BP250**, respectively. These compounds were prepared from the corresponding alkynyl resin incorporating

Peptide	Sequence
BP135	KKLFKK**X**$_a$KYL
BP136	KKLFKKI**X**$_a$YL
BP238	**X**$_b$KLFKKILKYL
BP239	**X**$_c$KLFKKILKYL
BP240	K**X**$_b$LFKKILKYL
BP241	K**X**$_c$LFKKILKYL
BP242	KKLF**X**$_b$KILKYL
BP243	KKLF**X**$_c$KILKYL
BP244	KKLFK**X**$_b$ILKYL
BP245	KKLFK**X**$_c$ILKYL
BP246	KKLFKKIL**X**$_b$YL
BP247	KKLFKKIL**X**$_c$YL
BP248	KKL**X**$_d$KKILKYL
BP249	KKL**X**$_e$KKILKYL
BP250	KKL**X**$_f$KKILKYL

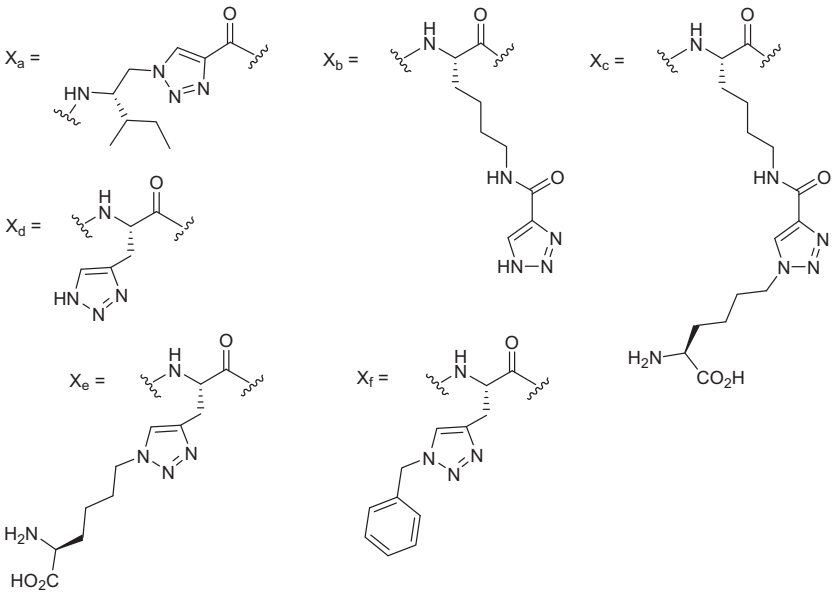

Fig. 1. Structure of the peptidotriazoles **BP135**, **BP136**, and **BP238**–**BP250**.

a propargylglycine at position 4 and treatment with NaN_3, Boc-Ahx(N_3)–OH or BnN_3 (Scheme 3).

Peptidotriazoles **BP238**–**BP250** are denoted as Lys^n(Tr), Lys^n(Tr-Ahx), Ala^4(Tr), Ala^4(Tr-Ahx) or Ala^4(Tr-Bn), where *n* is the position of the Lys residue that bears the triazole ring, Tr stands for an unsubstituted triazole, Tr-Ahx corresponds to a triazole substituted with a 2-aminohexanoic acid, and Tr-Bn is a triazole substituted with a benzyl group (Fig. 1, Table 1).

All peptidotriazoles were obtained in moderate to good RP-HPLC purities ranging from 65 to 98%, and were characterized by mass spectrometry (Table 1).

3.2. Antibacterial activity

Peptidotriazoles were tested for in vitro growth inhibition of *E. amylovora*, *P. syringae* pv. *syringae* and *X. axonopodis* pv. *vesicatoria* at 1.6, 3.1, 6.2, 12.5, 25, and 50 μM (Table 2). Peptides **BP135** (Ile^7-Tr) and **BP136** (Ile^8-Tr), incorporating a triazole ring at the backbone, were substantially less active than **BP100**. Only **BP136** displayed a moderate activity against *X. axonopodis* pv. *vesicatoria* (MIC of 12.5–25 μM).

By contrast, peptidotriazoles bearing a triazole ring at an amino acid side-chain were considerably active. Eleven out of thirteen sequences displayed MIC values <12.5 μM against the three pathogens. Peptidotriazoles **BP238**–**BP247** incorporating a Lys residue modified with a triazole exhibited higher activity against *X. axonopodis* pv. *vesicatoria* and *E. amylovora* than against *P. syringae* pv. *syringae*. Nine out of ten sequences displayed MIC values ranging from 1.6 to 6.2 μM against *X. axonopodis* pv. *vesicatoria*, being **BP245** the most active sequence. This peptide incorporated a triazole bearing a 2-aminohexanoic acid at residue 6 (Lys^6(Tr-Ahx)) (MIC of 1.6–3.1 μM), and showed a higher activity than **BP100** (MIC

Table 1
Sequences, retention times and purities on RP-HPLC, and HRMS data.

Peptide	Sequence[a]	Notation[b]	t_R (min)[c]	Purity[d] (%)	HRMS
BP135	KKLFKK**X**$_a$KYL	Ile^7-Tr	5.97[e]	98	463.6490 $[M+3H]^{3+}$, 694.9673 $[M+2H]^{2+}$
BP136	KKLFKKI**X**$_a$YL	Ile^8-Tr	6.17[e]	85	458.6440 $[M+3H]^{3+}$, 687.4622 $[M+2H]^{2+}$
BP238	**X**$_b$KLFKKILKYL	Lys^1(Tr)	17.70[f]	84	506.0014 $[M+3H]^{3+}$, 758.4946 $[M+2H]^{2+}$
BP239	**X**$_c$KLFKKILKYL	Lys^1(Tr-Ahx)	17.33[f]	73	549.0280 $[M+3H]^{3+}$, 823.0338 $[M+2H]^{2+}$
BP240	K**X**$_b$LFKKILKYL	Lys^2(Tr)	17.94[f]	84	506.0008 $[M+3H]^{3+}$, 758.4940 $[M+2H]^{2+}$
BP241	K**X**$_c$LFKKILKYL	Lys^2(Tr-Ahx)	17.67[f]	82	549.0295 $[M+3H]^{3+}$, 823.0358 $[M+2H]^{2+}$
BP242	KKLF**X**$_b$KILKYL	Lys^5(Tr)	17.85[f]	79	506.0025 $[M+3H]^{3+}$
BP243	KKLF**X**$_c$KILKYL	Lys^5(Tr-Ahx)	17.48[f]	92	549.0300 $[M+3H]^{3+}$, 823.0352 $[M+2H]^{2+}$
BP244	KKLFK**X**$_b$ILKYL	Lys^6(Tr)	17.85[f]	84	506.0015 $[M+3H]^{3+}$
BP245	KKLFK**X**$_c$ILKYL	Lys^6(Tr-Ahx)	17.43[f]	81	549.0288 $[M+3H]^{3+}$
BP246	KKLFKKIL**X**$_b$YL	Lys^9(Tr)	17.51[f]	72	506.0034 $[M+3H]^{3+}$, 758.4979 $[M+2H]^{2+}$
BP247	KKLFKKIL**X**$_c$YL	Lys^9(Tr-Ahx)	17.16[f]	71	549.0289 $[M+3H]^{3+}$, 823.0373 $[M+2H]^{2+}$
BP248	KKL**X**$_d$KKILKYL	Ala^4(Tr)	15.82[f]	76	471.3279 $[M+3H]^{3+}$, 706.4847 $[M+2H]^{2+}$
BP249	KKL**X**$_e$KKILKYL	Ala^4(Tr-Ahx)	15.69[f]	65	514.3538 $[M+3H]^{3+}$, 771.0215 $[M+2H]^{2+}$
BP250	KKL**X**$_f$KKILKYL	Ala^4(Tr-Bn)	16.91[f]	91	501.3431 $[M+2H]^{3+}$

[a] All peptides are C-terminal amides (see structures in Fig. 1).
[b] The notation defines the variation at the **X** position indicated as superscript. Ile-Tr stands for Ile-Ψ[CH_2triazoleCO]. For peptides BP238–BP250 the side chain substituent of the Lys or the Ala residue is in parenthesis being: Tr, unsubstituted triazole; Tr-Ahx, triazole bearing a 2-aminohexanoic acid; Tr-Bn, triazole bearing a benzyl group.
[c] RP-HPLC retention time.
[d] Percentage determined by RP-HPLC at 220 nm from the crude reaction mixture.
[e] RP-HPLC analysis using method A (see Section 2).
[f] RP-HPLC analysis using method B (see Section 2).

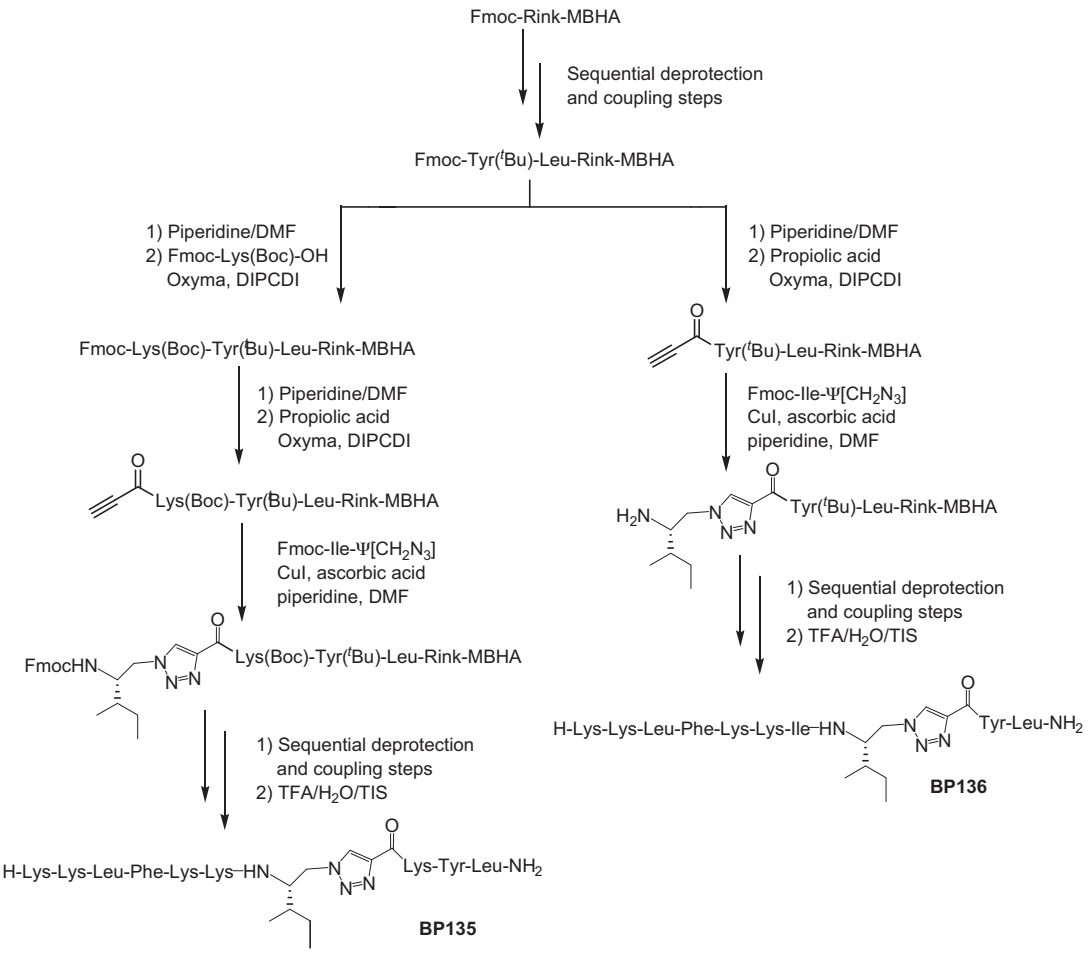

Scheme 1. Synthesis of peptidotriazoles **BP135** and **BP136** bearing a triazole moiety in the peptide backbone.

of 3.1–6.2 μM). **BP247** (Lys^9(Tr-Ahx)) was the least active against this pathogen with a MIC of 6.2–12.5 μM. Against *E. amylovora* seven peptides displayed MIC values ranging from 1.6 to 6.2 μM, being **BP246** (Lys^9(Tr)) and **BP247** (Lys^9(Tr-Ahx)) more active than **BP100** (MIC of 1.6–3.1 vs. 3.1–6.2 μM). **BP240** (Lys^2(Tr)), **BP241** (Lys^2(Tr-Ahx)) and **BP242** (Lys^5(Tr)) showed the lowest activity (MIC of 6.2–12.5 μM). Three peptides, **BP243** (Lys^5(Tr-Ahx)), **BP244** (Lys^6(Tr)) and **BP247** (Lys^9(Tr-Ahx)), exhibited MIC values ranging from 3.1 to 6.2 μM against *P. syringae* pv. *syringae*, and were as active as **BP100**.

Peptidotriazoles **BP248**–**BP250**, bearing a triazole instead of a benzene ring at the Phe residue in **BP100**, displayed a higher activity

Table 2
Antibacterial activity (MIC) against three plant pathogenic bacteria and fungi, cytotoxicity and stability to protease degradation.

Peptide[a]	MIC (μM)					Hemolysis[c] (%)		Digestion[d] (%)
	Xav[b]	*Ea*[b]	*Pss*[b]	*Pe*[b]	*Fo*[b]	50 μM	150 μM	
BP100	3.1–6.2	3.1–6.2	3.1–6.2	25–50	<6.2	3 ± 0.1	22 ± 2.8	76
BP135	25–50	25–50	>50	>50	25–50	1 ± 0.44	1 ± 0.26	5
BP136	12.5–25	>50	>50	>50	>50	0 ± 0.12	0 ± 0.12	7
BP238	3.1–6.2	3.1–6.2	6.2–12.5	25–50	<6.2	23 ± 2.6	43 ± 4.0	79
BP239	3.1–6.2	3.1–6.2	6.2–12.5	25–50	<6.2	14 ± 1.2	30 ± 1.2	73
BP240	3.1–6.2	6.2–12.5	6.2–12.5	25–50	<6.2	34 ± 2.1	57 ± 1.2	64
BP241	3.1–6.2	6.2–12.5	6.2–12.5	25–50	<6.2	1 ± 1.0	6 ± 1.2	59
BP242	3.1–6.2	6.2–12.5	6.2–12.5	25–50	6.2–12.5	39 ± 2.9	62 ± 5.5	91
BP243	3.1–6.2	3.1–6.2	3.1–6.2	25–50	<6.2	10 ± 1.5	22 ± 4.7	100
BP244	3.1–6.2	3.1–6.2	3.1–6.2	25–50	<6.2	37 ± 0.9	73 ± 2.0	93
BP245	1.6–3.1	3.1–6.2	6.2–12.5	25–50	<6.2	21 ± 0.5	54 ± 1.2	97
BP246	3.1–6.2	1.6–3.1	6.2–12.5	>50	6.2–12.5	48 ± 1.3	75 ± 4.7	55
BP247	6.2–12.5	1.6–3.1	3.1–6.2	>50	6.2–12.5	20 ± 0.7	38 ± 3.4	91
BP248	6.2–12.5	12.5–25	3.1–6.2	>50	6.2–12.5	1 ± 0.1	1 ± 0.2	79
BP249	25–50	>50	12.5–25	>50	6.2–12.5	0 ± 0.2	0 ± 0.7	70
BP250	6.2–12.5	3.1–6.2	1.6–3.1	>50	6.2–12.5	0 ± 0.1	0 ± 0.5	62

[a] All peptides are C-terminal amides (see structures in Fig. 1).
[b] *Xav*, *Xanthomonas axonopodis* pv. *vesicatoria*; *Ea*, *Erwinia amylovora*; *Pss*, *Pseudomonas syringae pv. syringae*; *Pe*, *Penicillium expansum*; *Fo*, *Fusarium oxysporum*.
[c] Percent hemolysis at 50 and 150 μM plus confidence interval ($\alpha = 0.05$).
[d] Percentage of degraded peptide calculated by RP-HPLC after 1 h.

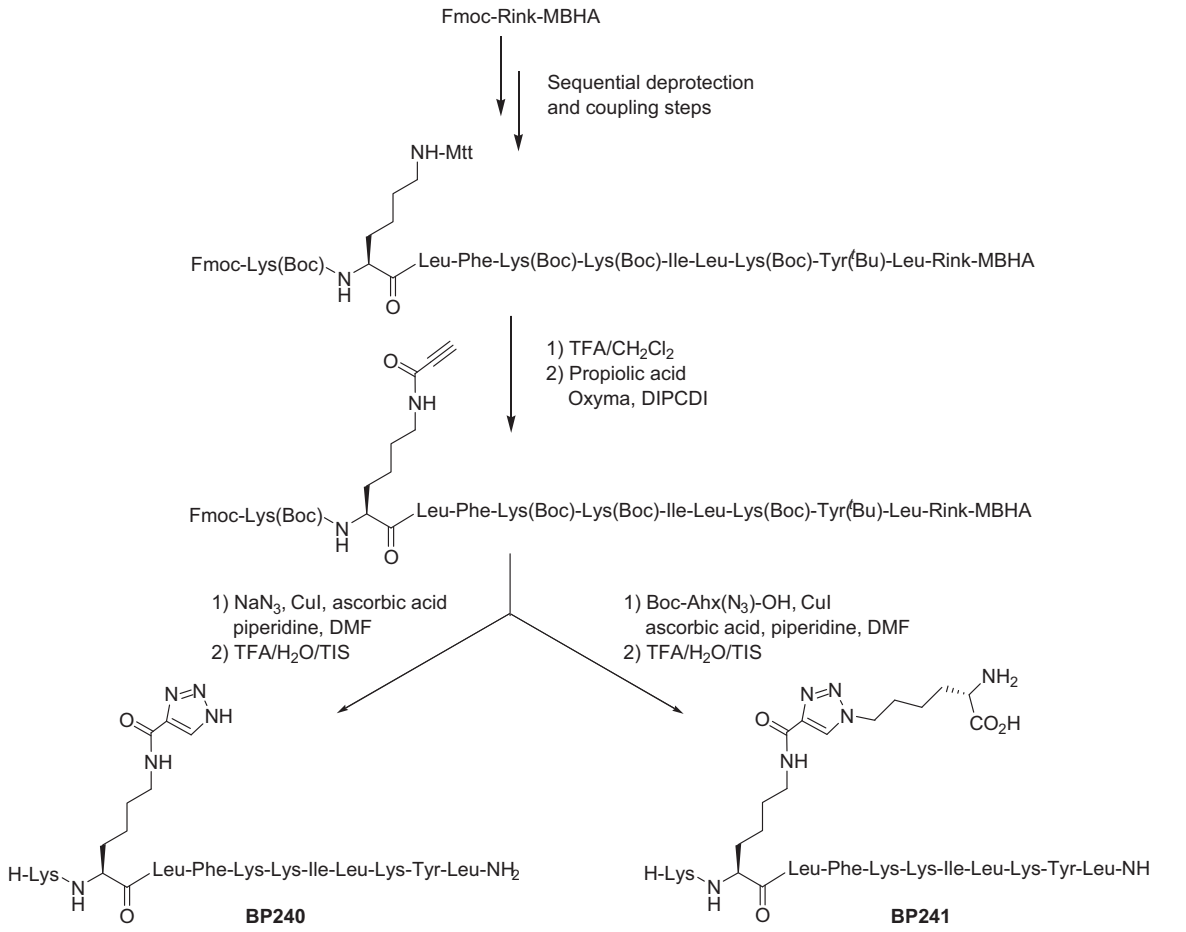

Scheme 2. General strategy for the synthesis of peptidotriazoles **BP238**–**BP247** bearing a triazole moiety at the side-chain of a Lys residue as shown for **BP240** and **BP241**.

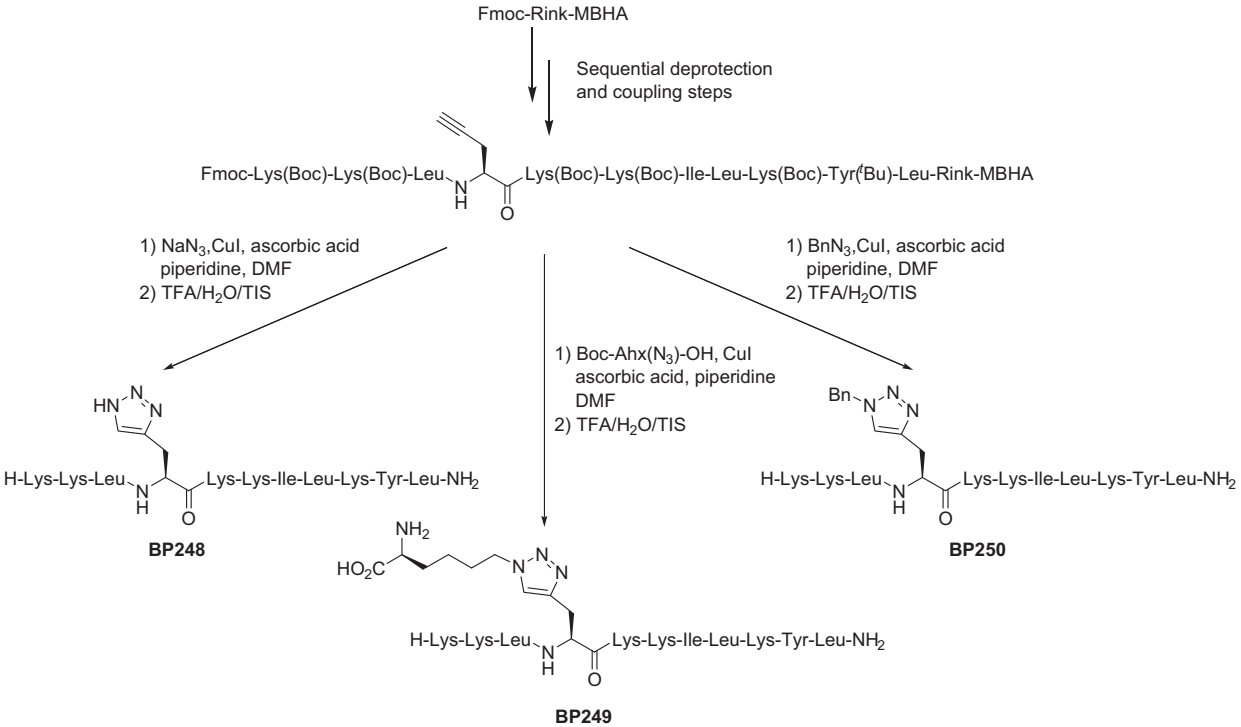

Scheme 3. Synthesis of peptidotriazoles **BP248**, **BP249** and **BP250** bearing a triazole moiety at the side-chain of an Ala residue.

against *P. syringae* pv. *syringae* (MIC of 1.6–25 μM) than against the other two pathogens (MIC of 3.1 to >50 μM). **BP250** (Ala^4(Tr-Bn)) was the most active of these three sequences (MIC of 1.6–12.5 μM), being more active than **BP100** against *P. syringae* pv. *syringae* (MIC of 1.6–3.1 vs. 3.1–6.2 μM). **BP248** (Ala^4(Tr)) showed a slightly lower activity (MIC of 3.1–25 μM) as compared to **BP250** and was as active as **BP100** against *P. syringae* pv. *syringae* (MIC of 3.1–6.2 μM). The analog incorporating a 2-aminohexanoic acid substituent at the triazole ring, **BP249** (Ala^4(Tr-Ahx)), was the least active with MIC values ranging from 12.5 to >50 μM.

3.3. Antifungal activity

The antifungal activity of the peptidotriazoles was screened in vitro against *P. expansum* and *F. oxysporum* at 6.2, 12.5, 25 and 50 μM (Table 2). Peptidotriazoles were poorly active against *P. expansum*. Only eight sequences incorporating a Lys residue modified with a triazole showed MICs ranging from 25 to 50 μM. In contrast, *F. oxysporum* was particularly sensitive to peptidotriazoles. Seven sequences exhibited MICs < 6.2 μM and six displayed antifungal activity within 6.2 and 12.5 μM. Best peptides also were from the set bearing a triazole at a Lys side-chain and displayed similar activity than **BP100**.

3.4. Hemolytic activity

The toxicity to eukaryotic cells of peptidotriazoles was determined as the ability to lyse erythrocytes in comparison to melittin. Percent hemolysis at 50 and 150 μM is shown in Table 2. Peptidotriazoles **BP135** (Ile^7-Tr), **BP136** (Ile^8-Tr), **BP241** (Lys^2(Tr-Ahx)), **BP248** (Ala^4(Tr)), **BP249** (Ala^4(Tr-Ahx)), and **BP250** (Ala^4(Tr-Bn)) showed ≤6% hemolysis at 150 μM. Among the set of peptidotriazoles bearing a triazole at a Lys side-chain, **BP239** and **BP243** displayed a hemolytic activity similar to **BP100** at 150 μM (30 and 22%, respectively). Moreover, the sequences incorporating a triazole substituted with a 2-aminohexanoic acid (**BP239**, **BP241**, **BP243**, **BP245**, and **BP247**) were less hemolytic than the unsubstituted counterparts (**BP238**, **BP240**, **BP242**, **BP244**, and **BP246**), 0.6–21% vs. 23–48% at 50 μM.

3.5. Cytoxicity of peptidotriazoles against tobacco leaves

The toxicity of all peptidotriazoles against tobacco leaves was assessed by infiltrating 100 μL of a 25 and 50 μM solution of each compound into the mesophylls of the leaves (Fig. S1, Supporting information). As positive control, the nonspecific and nonselective peptide mellitin was used. After 48 h of infiltration, a brown necrotic area was observed for this peptide. In contrast, no necrosis could be detected in the mesophylls of the leaves that were infiltrated with the peptidotriazoles.

3.6. Susceptibility to protease degradation

The susceptibility of the peptides to proteolysis was studied by exposure to proteinase K and degradation was monitored by RP-HPLC over time (Table 2). Peptides **BP135** (Ile^7-Tr) and **BP136** (Ile^8-Tr), incorporating a triazole ring at the backbone, were degraded less than 10% after 1 h incubation, being substantially more stable than **BP100**. Among the set of sequences bearing a triazole ring at an amino acid side-chain, **BP240** (Lys^2(Tr)), **BP241** (Lys^2(Tr-Ahx)), **BP246** (Lys^9(Tr)), and **BP250** (Ala^4(Tr-Bn)) displayed higher stability than **BP100** (55–64% degradation). Moreover, peptidotriazoles **BP238** (Lys^1(Tr)), **BP239** (Lys^1(Tr-Ahx)), **BP248** (Ala^4(Tr)), **BP249** (Ala^4(Tr-Ahx)) displayed similar susceptibility to protease degradation than **BP100**, and after 1 h incubation only 70–79% degradation was observed.

4. Discussion

As part of our search for effective agents to control the plant pathogenic bacteria *X. axonopodis* pv. *vesicatoria*, *E. amylovora* and *P. syringae* pv. *syringae*, and the phytopathogenic fungi *P. expansum* and *F. oxysporum*, we have previously identified undecapeptides with interesting biological properties [4,5,14]. In particular, **BP100**, consisting of LysLysLeuPheLysLysIleLeuLysTyrLeu-NH_2, exhibited high activity against the phytopathogenic bacteria at similar concentrations than conventional antibiotics, displayed low cytotoxicity, and showed significant stability toward protease degradation. These promising results prompted us to design new analogs bearing a 1,2,3-triazole ring. This heterocycle has been shown to be a crucial motif in biologically active compounds due to its stability to metabolic degradation, its high dipole moment and its ability to participate in hydrogen bonding. Taking into account these properties, we investigated the influence of incorporating a 1,2,3-triazole ring in the backbone of **BP100**. Moreover, we analyzed the effect of modifying the side chain of each Lys and of the Phe in **BP100** with a triazole moiety as well as the influence of introducing a substituent in the triazole ring.

The evaluation of the antibacterial activity showed that the introduction of a triazole ring in the peptide backbone resulted in a decrease of the activity, peptidotriazoles **BP135** and **BP136** were the least active sequences. On the contrary, in general, peptidotriazoles **BP238**–**BP250** incorporating a triazole onto a side-chain of a Phe or a Lys exhibited similar activity than the parent peptide, with eleven sequences displaying MIC <12.5 μM against the three pathogens. These results suggest that the conformational restrictions imposed by the introduction of a triazole in the peptide backbone impede the adoption of the secondary structure necessary for the activity of this type of antimicrobial peptides [5].

A different susceptibility of bacteria to the two sets of peptidotriazoles **BP238**–**BP247** and **BP248**–**BP250** was observed. Peptidotriazoles **BP238**–**BP247** bearing a triazole at a Lys side chain were more active against *X. axonopodis* pv. *vesicatoria* and *E. amylovora* (MIC of 1.6–12.5 μM) than against *P. syringae* pv. *syringae*. In contrast, when the benzene ring of the Phe was replaced by a triazole, the corresponding peptidotriazoles **BP248**–**BP250** were more active against *P. syringae* pv. *syringae* (MIC of 1.6–25 μM) than against the other two bacteria. This differential susceptibility of bacteria to a given peptide has been attributed to differences in the membrane components of the target microorganism, e.g. charge and lipid composition, that would influence rates of binding of peptides to the membrane [20].

The analysis of the effect of introducing a substituent in the triazole ring revealed that, for the set of peptidotriazoles **BP238**–**BP247**, this substitution did not significantly influence the antibacterial activity. In fact, the sequences bearing an unsubstituted triazole displayed MIC values similar to that of the corresponding counterpart bearing a triazole substituted with a 2-aminohexanoic acid. Moreover, the activity of these derivatives did not differ from that of the parent sequence **BP100**, suggesting that the triazole ring does not modify the peptide hydrophilicity. The more sensitive positions to the introduction of the substituent were Lys^5, Lys^6 and Lys^9. Substitution of the triazole at Lys^5 led to **BP243** (Lys^5(Tr-Ahx)) with higher activity against *E. amylovora* and *P. syringae* pv. *syringae* than the unsubstituted counterpart **BP242** (Lys^5(Tr)). The activity against *P. syringae* pv. *syringae* was also enhanced when a 2-aminohexanoic acid was introduced at Lys^9 (**BP246** vs. **BP247**). Against *X. axonopodis* pv. *vesicatoria* the peptidotriazole **BP245** bearing a substituted triazole at Lys^6 was more

active than the unsubstituted analog **BP244**. Interestingly, peptidotriazoles **BP245** (Lys^6(Tr-Ahx)), **BP246** (Lys^9(Tr)) and **BP247** (Lys^9(Tr-Ahx)) exhibited higher activity than **BP100** against *X. axonopodis* pv. *vesicatoria* and *E. amylovora* (MIC of 1.6–3.1 μM).

The analysis of the antibacterial activity of peptidotriazoles **BP248**–**BP250**, in which the benzene ring of Phe^4 in **BP100** was replaced by a triazole, pointed out that the hydrophobicity at this position is crucial. In fact, the analog incorporating a triazole substituted with a 2-aminohexanoic acid (**BP249**) was the least active, whereas the peptidotriazole bearing a benzyl group at the triazole (**BP250**) was the most active, with higher activity than **BP100** against *P. syringae* pv. *syringae* (MIC of 1.6–3.1 μM).

The antifungal activity of the peptidotriazoles correlated with that previously reported for structurally related undecapeptides, which showed that *F. oxysporum* was more susceptible than *P. expansum* to these compounds [4]. As for antibacterial activity, the introduction of a triazole at the peptide backbone resulted in sequences not active against these fungi. Peptidotriazoles **BP238**–**BP247**, bearing a triazole at a Lys side chain, were more active than those including a triazole ring at position 4 (**BP248**–**BP250**), being the best derivatives as active as **BP100**. Moreover, the incorporation of a substituent in the triazole ring did not influence the antifungal activity.

Peptidotriazole cytotoxicity was also strongly influenced by the amino acid (Lys or Phe) that was modified with a triazole as well as by the absence or presence of a substituent in this heterocyclic ring. Peptidotriazoles resulting from the modification of the Phe^4 were less hemolytic than those obtained from the incorporation of a triazole at a Lys side chain. For the former (**BP248**–**BP250**), the replacement of the benzene ring by a triazole, either substituted or unsubstituted, rendered sequences with a lower hydrophobic character than that of **BP100**, being not hemolytic even at 150 μM. For the derivatives incorporating a triazole at a Lys side chain (**BP238**–**BP247**), the least hemolytic sequences were those bearing a 2-aminohexanoic acid substituent (0.6–21% at 50 μM). In this case, the presence of this substituent also decreases the hydrophobic character of the triazole moiety. However, these sequences were more hemolytic than **BP100** suggesting that the triazole ring confers a higher hydrophobic character than the free ε-amino group of a Lys. These results are in good agreement with previous studies on antimicrobial peptides reporting that an increase of the peptide hydrophobicity is related to an increase in the cytotoxicity [7,36]. Peptides with an optimal balance between antibacterial and hemolytic activities were **BP238**, **BP239**, **BP243**, **BP245**, **BP247**, and **BP250**. Among them, **BP238**, **BP239**, **BP243**, and **BP245** also showed high antifungal activity. In addition, we examined the toxicity of the peptidotriazoles against tobacco leaves. In contrast to mellitin which severely damaged the leaf mesophyll tissues, these compounds did not induce any phytotoxicity.

Protease digestion stability is a desired property in antimicrobial peptides to assure a reasonable half-life of the molecule in the plant environment. Proteases from epiphytic microorganisms or intrinsic to the plant in internal tissues may degrade antimicrobial peptides [2,9]. The incorporation of a triazole moiety at the peptide backbone strongly increased the stability to protease digestion. The modification of Lys^5 and Lys^6 with an unsubstituted or substituted triazole as well as the incorporation of a triazole substituted with a 2-aminohexanoic acid at Lys^9 afforded the least stable peptidotriazoles (**BP242**–**BP245** and **BP247**). The rest of sequences showed similar protease susceptibility than that of the parent peptide **BP100**. Peptidotriazoles with a good biological profile, **BP238**, **BP239**, and **BP250**, also showed good stability toward protease degradation. Especially noteworthy is **BP250** that is active against the three bacteria, not hemolytic and more stable to proteases than **BP100**.

In summary, we have designed and synthesized **BP100** analogs containing a triazole ring. The introduction of this moiety at a Lys or a Phe side chain has led to the identification of sequences active against *X. axonopodis* pv. *vesicatoria*, *E. amylovora*, *P. syringae* pv. *syringae*, and *F. oxysporum* with low hemolytic activity, high stability to protease digestion and no phytotoxicity, being good candidates to design new antimicrobial agents. Efficacy tests with selected peptidotriazoles in pathogen inoculated host plants are under progress to confirm their potential as plant protection products.

Acknowledgments

Imma Güell was recipient of a predoctoral fellowship from the Generalitat de Catalunya. This work was supported by grant AGL2009-13255-C02-02/AGR from MICINN of Spain. We also acknowledge the Serveis Tècnics de Recerca of the University of Girona for the ESI-MS analysis.

Appendix A. Supplementary data

Supplementary data associated with this article can be found, in the online version, at doi:10.1016/j.peptides.2011.12.003.

References

[1] Agrios GN. Plant Pathology. 4th ed. California: Academic Press; 1998.
[2] Ali GS, Reddy ASN. Inhibition of fungal and bacterial plant pathogens by synthetic peptides: in vitro growth inhibition, interaction between peptides, and inhibition of disease progression. Mol Plant-Microbe Interact 2000;13:847–59.
[3] Aufort M, Herscovici J, Bouhours P, Moreau N, Girard C. Synthesis antibiotic activity of a small molecules library of 1,2,3-triazole derivatives. Bioorg Med Chem Lett 2008;18:1195–8.
[4] Badosa E, Ferre R, Francés J, Bardají E, Feliu L, Planas M, Montesinos E. Sporicidal activity of synthetic antifungal undecapeptides and control of penicillium rot of apples. Appl Environ Microbiol 2009;75:5563–9.
[5] Badosa E, Ferre R, Planas M, Feliu L, Besalú E, Cabrefiga J, Bardají E, Montesinos E. A library of linear undecapeptides with bactericidal activity against phytopathogenic bacteria. Peptides 2007;28:2276–85.
[6] Bechinger B, Lohner K. Detergent-like actions of linear amphipathic cationic antimicrobial peptides. Biochim Biophys Acta 2006;1758:1529–39.
[7] Blondelle SE, Lohner K. Combinatorial libraries: a tool to design antimicrobial and antifungal peptide analogues having lytic specificities for structure–activity relationship studies. Biopolymers 2000;55:74–87.
[8] Cantel S, Isaad AC, Scrima M, Levy JJ, DiMarchi RD, Rovero P, Halperin JA, D'Ursi AM, Papini AM, Synthesis Chorev M. conformational analysis of a cyclic peptide obtained via *i* to *i* + 4 intramolecular side-chain to side-chain azide–alkyne 1,3-dipolar cycloaddition. J Org Chem 2008;73:5663–74.
[9] Cavallarin L, Andreu D, San Segundo B. Cecropin A-derived peptides are potent inhibitors of fungal plant pathogens. Mol Plant-Microbe Interact 1998;11:218–27.
[10] Chakrabarty SP, Ramapanicker R, Mishra R, Chandrasekaran S, Balaram H. Development and characterization of lysine based tripeptide analogues as inhibitors of sir2 activity. Bioorg Med Chem 2009;17:8060–72.
[11] Chassaing S, Sani Souda Sido A, Alix A, Kumarraja M, Pale P, Sommer J. Click chemistry in zeolites: copper(I) zeolites as new heterogeneous and ligand-free catalysts for the Huisgen [3+2] cycloaddition. Chem Eur J 2008;14:6713–21.
[12] Evans RA. The rise of azide–alkyne 1,3-dipolar 'Click' cycloaddition and its application to polymer science and surface modification. Aust J Chem 2007;60:384–95.
[13] Fan WQ, Katritzky AR. In: Katritzky AR, Rees CW, Scriven VEFB, editors. Comprehensive Heterocyclic Chemistry II, vol. 4. Oxford: Elsevier Science; 1996. p. 1–126.
[14] Ferre R, Badosa E, Feliu L, Planas M, Montesinos E, Bardají E. Inhibition of plant-pathogenic bacteria by short synthetic cecropin A-melittin hybrid peptides. Appl Environ Microbiol 2006;72:3302–8.
[15] Franke R, Doll C, Eichler J. Peptide ligation through click chemistry for the generation of assembled and scaffolded peptides. Tetrahedron Lett 2005;46:4479–82.
[16] Güell I, Cabrefiga J, Badosa E, Ferre R, Talleda M, Bardají E, Planas M, Feliu L, Montesinos E. Improvement of the efficacy of linear undecapeptides against plant pathogenic bacteria by incorporating D-amino acids. Appl Environ Microbiol 2011;77:2667–75.
[17] Hancock REW, Sahl HG. Antimicrobial and host defense peptides as new anti-infective therapeutic strategies. Nature Biotechnol 2006;24:1551–7.
[18] Hein JE, Fokin VV. Copper-catalyzed azide–alkyne cycloaddition (CuAAC) and beyond: new reactivity of copper(I) acetylides. Chem Soc Rev 2010;39:1302–15.

[19] Holub JM, Kirshenbaum K. Tricks with clicks: modification of peptidomimetic oligomers via copper-catalyzed azide–alkyne [3+2] cycloaddition. Chem Soc Rev 2010;39:1325–37.
[20] Huang HW. Action of antimicrobial peptides: two-state model. Biochemistry 2000;39:8347–52.
[21] Huang HW. Molecular mechanism of antimicrobial peptides: the origin of cooperativity. Biochim Biophys Acta 2006;1758:1292–302.
[22] Jagasia R, Holub JM, Bollinger M, Kirshenbaum K, Finn MG. Peptide cyclization and cyclodimerization by CuI-mediated azide–alkyne cycloaddition. J Org Chem 2009;74:2964–74.
[23] Jølck RI, Berg RH, Andresen TL. Solid-phase synthesis of PEGylated lipopeptides using click chemistry. Bioconjugate Chem 2010;21:807–10.
[24] Keymanesh K, Soltani S, Sardari S. Application of antimicrobial peptides in agriculture and food industry. World J Microbiol Biotechnol 2009;25:933–44.
[25] Liu Y, Zhang L, Wang J, Li Y, Xu Y, Pan Y. Design and synthesis of cyclo[-Arg-Gly-Asp-Ψ(triazole)-Gly-Xaa-] peptide analogues by click chemistry. Tetrahedron 2008;64:10728–34.
[26] Loper JE, Henkels MD, Roberts RG, Grove GG, Willet MJ, Smith TJ. Evaluation of streptomycin, oxytetracycline and copper resistance of *Erwinia amylovora* isolated from pear orchards in Washington state. Plant Dis 1991;75:287–90.
[27] Mamidyala SK, Finn MG. In situ click chemistry: probing the binding landscapes of biological molecules. Chem Soc Rev 2010;39:1252–61.
[28] Marcos JF, Gandía M. Antimicrobial peptides: to membranes and beyond. Expert Opin Drug Discov 2009;4:659–71.
[29] Marcos JF, Muñoz A, Pérez-Payá E, Misra S, López-García B. Identification and rational design of novel antimicrobial peptides for plant protection. Annu Rev Phytopathol 2008;46:271–301.
[30] McManus PS, Stockwell VO, Sundin VO, Jones AL. Antibiotic use in plant agriculture. Annu Rev Phytopathol 2002;40:443–65.
[31] Meldal M, Tornøe CW. Cu-catalyzed azide–alkyne cycloaddition. Chem Rev 2008;108:2952–3015.
[32] Mondal S, Fan E. Mild and efficient synthesis of Fmoc-protected amino azides from Fmoc-protected amino alcohols. Synlett 2006:306–8.
[33] Montesinos E. Antimicrobial peptides and plant disease control. FEMS Microbiol Lett 2007;270:1–11.
[34] Montesinos E, Bardají E. Synthetic antimicrobial peptides as agricultural pesticides for plant-disease control. Chem Biodivers 2008;5:1225–37.
[35] Moses JE, Moorhouse AD. The growing applications of click chemistry. Chem Soc Rev 2007;36:1249–62.
[36] Oh D, Shin SY, Lee S, Kang JH, Kim SD, Ryu PD, Hahm KS, Kim Y. Role of the hinge region and the tryptophan residue in the synthetic antimicrobial peptides, cecropin A(1–8)-magainin 2(1–12) and its analogues, on their antibiotic activities and structures. Biochemistry 2000;39:11855–64.
[37] Reck F, Zhou F, Girardot M, Kern G, Eyermann CJ, Hales NJ, Ramsay RR, Gravestock MB. Identification of 4-substituted 1,2,3-triazoles as novel oxazolidinone antibacterial agents with reduced activity against monoamine oxidase A. J Med Chem 2005;48:499–506.
[38] Rodriguez M, Linares M, Doulut S, Heitz A, Martinez J. A facile synthesis of chiral n-protected amino alcohols. Tetrahedron Lett 1991;32:923–6.
[39] Scrima M, Chevalier-Isaad A, Rovero P, Papini AM, Chorev M, D'Ursi AM. Cu^{I}-catalyzed azide–alkyne intramolecular i-to-(i + 4) side-chain-to-side-chain cyclization promotes the formation of helix-like secondary structures. Eur J Org Chem 2010:446–57.
[40] Springer J, de Cuba KR, Calvet-Vitale A, Geenevasen JAJ, Hermkens PHH, Hiemstra H, van Maarseveen JH. Backbone amide linker strategy for the synthesis of 1,4-triazole-containing cyclic tetra- and pentapeptides. Eur J Org Chem 2008:2592–600.
[41] Sundin GW, Ecological Bender CL. genetic analysis of copper and streptomycin resistance in *Pseudomonas syringae* pv *syringae*. Appl Environ Microbiol 1993;59:1018–24.
[42] Sureshbabu VV, Narendra N, Hemantha HP, Chennakrishnareddy G. Click chemistry aided synthesis of 1,4- substituted 1,2,3-triazole linked N-Fmoc protected triazole-amino acids: Isolation, characterization and synthesis of novel triazole based amino free unnatural amino acids. Protein Peptide Lett 2010;17:499–506.
[43] Tornøe CW, Christensen C, Meldal M. Peptidotriazoles on solid phase: [1,2,3]-triazoles by regiospecific copper(I)-catalyzed 1,3-dipolar cycloadditions of terminal alkynes to azides. J Org Chem 2002;67:3057–64.
[44] Tornøe CW, Sanderson SJ, Mottram JC, Coombs GH, Meldal M. Combinatorial library of peptidotriazoles: identification of [1,2,3]-triazole inhibitors against a recombinant Leishmania mexicana cysteine protease. J Comb Chem 2004;6:312–24.
[45] Tron GC, Pirali T, Billington RA, Canonico PL, Sorba G, Genazzani AA. Click chemistry reactions in medicinal chemistry: applications of the 1,3-dipolar cycloaddition between azides and alkynes. Med Res Rev 2008;28:278–308.
[46] Vidaver AK. Uses of antimicrobials in plant agriculture. Clin Infect Dis 2002;34:S107–10.
[47] Wan Q, Chen J, Chen G, Danishefsky SJ. A potentially valuable advance in the synthesis of carbohydrate-based anticancer vaccines through extended cycloaddition chemistry. J Org Chem 2006;71:8244–9.
[48] Whiting M, Muldoon J, Lin YC, Silverman SM, Lindstrom W, Olson AJ, Kolb HC, Finn MG, Sharpless KB, Elder JH, Fokin VV. Inhibitors of HIV-1 protease by using in situ click chemistry. Angew Chem Int Ed 2006;45:1435–9.